Review

Not peer-reviewed version

Advanced Dual-Wavelength and Dual-Frequency VECSEL Architectures: Design Principles and Application-Driven Performance Metrics

Léa Chaccour *

Posted Date: 3 April 2026

doi: 10.20944/preprints202604.0253.v1

Keywords: optically pumped VECSEL; dual-frequency VECSEL; dual-wavelength VECSE

 doi:10.20944/preprints202604.0253.v1

Review

Advanced Dual-Wavelength and Dual-Frequency VECSEL Architectures: Design Principles and Application-Driven Performance Metrics

Léa Chaccour [1,2]

[1] PITC, Eindhoven University of Technology (TU/e): De Groene Loper 19, 5612 AP- Eindhoven—The Netherlands; l.chaccour@tue.nl

[2] Photonic Integration Group, Eindhoven University of Technology (TU/e): De Groene Loper 19, 5612 AP-Eindhoven—The Netherlands

Abstract

Vertical-External-Cavity Surface-Emitting Lasers (VECSELs) have gained significant attention over the past two decades due to their versatility in a wide range of photonic applications. This review focuses on VECSEL configurations for dual-wavelength emission, highlighting their use in high-resolution spectroscopy, terahertz (THz) generation, and advanced optical communication. We explore recent developments in VECSEL designs, including systems utilizing birefringent crystals for polarization-based frequency separation and configurations with dual VECSEL chips or dual gain regions within a single cavity. These two-wavelength VECSELs enable diverse operation modes, including narrow-linewidth, pulsed, multimode, and frequency-converted emission, with high-brightness output, excellent beam quality, and tunable wavelengths. Additionally, the review discusses advancements in dual-frequency VECSELs, with applications in LIDAR systems for environmental monitoring, highly stable optical clocks, and fiber sensors. We examine improvements in cavity design, semiconductor structures, and power stabilization, which have enhanced frequency stability and spectral purity, making VECSELs suitable for precision metrology and sensing applications.

Keywords: optically pumped VECSEL; dual-frequency VECSEL; dual-wavelength VECSEL

1. Introduction

The invention of lasers has led to a growing range of applications that leverage their unique advantages, driving advancements across science, industry, and medicine. This progress has been fueled by developments in semiconductor technology, miniaturization, and the diversification of gain materials, enabling more compact devices, higher efficiencies, and greater wavelength versatility [1].

Semiconductor lasers, are compact and efficient light sources that operate based on the principle of stimulated emission. They are widely used in modern technology, playing a crucial role in everyday life through applications such as optical communication, medical imaging, and consumer electronics [2]. These lasers have significantly impacted everyday life, particularly through their integration into optical devices. Due to their compact size, efficiency, and ease of integration, electrically pumped semiconductor lasers have become widely used in telecommunications applications. Their ability to provide stable and reliable light sources has contributed to their increasing popularity in advanced optical communication systems. Typically, these lasers fall into two main categories: edge emitters, which utilize a p-i-n junction with in-plane gain, and surface emitters, such as vertical-cavity surface-emitting lasers (VCSELs), which feature normal-to-plane emission [2].

 doi:10.20944/preprints202604.0253.v1

Vertical-External-Cavity-Surface-Emitting-Lasers (VECSELs) share their fundamental structure with surface-emitting semiconductor microcavity lasers [2]. However, unlike conventional VCSELs, they incorporate an external resonator, enhancing their performance. Their open-cavity architecture further enhances their potential across diverse applications, such as passive mode locking, which has been demonstrated to be capable of generating ultrashort pulses [3], multi-GHz repetition rates [4], and high average and peak pulse power [5,6]. This hybrid design merges the advantages of solid-state and gas lasers, offering high-brightness, high-beam-quality light sources across various wavelengths [7].

Optically pumped VECSELs, also known as optically pumped semiconductor lasers (OPSLs)-enable high-power operation, with output powers exceeding 100W demonstrated in 2012 [8]. First realized in 1997 [9], they continue to evolve as versatile light sources due to their flexible design and functional adaptability.

In this paper, we explore the design of dual-wavelength VECSELs, ranging from single-cavity configurations utilizing spectral hole burning to dual-chip systems for independent wavelength generation. We further delve into dual-frequency architectures that employ birefringent crystals to generate closely spaced frequencies for sensing applications. We conclude that the integration of these dual-mode chips into ruggedized architectures facilitates a transition from laboratory prototypes to 'semiconductor bricks', integrated, field-deployable units capable of replacing complex optical benches in 6G infrastructure and space-based metrology.

2. VECSEL Operation

The core component of a VECSEL is a semiconductor chip, precisely grown using epitaxy techniques like Metal-Organic Vapor-Phase-Epitaxy (MOVPE) or Molecular-Beam-Epitaxy (MBE). This chip consists of an active semiconductor region, a cap layer, and a highly reflective Bragg mirror. The emission wavelength is primarily determined by the semiconductor material's band-gap energy. The spectral gain-cavity detuning, a key property of VECSEL chips, can be engineered to enhance the device's output power. It refers to the spectral gap between the sub-cavity resonance, where the standing light field's anti-nodes align with the QW positions, and the material's gain spectrum [10].

To operate, optically pumped VECSELs, typically use a high-power, low-cost pump laser directed at an oblique angle, or, less commonly, electrical pumping via a doped p-i-n structure. Optical pumping is generally preferred due to its ability to provide high brightness, uniform charge-carrier excitation, and the absence of light-absorbing dopants, which can affect performance [7]. The laser resonator is completed with external mirrors, including at least one essential out-coupling mirror that enables mode oscillation and gain while defining the optical output (Figure 1). This design allows VECSELs to maintain excellent beam quality despite the low-quality pump beam, thanks to the vertical external cavity structure.

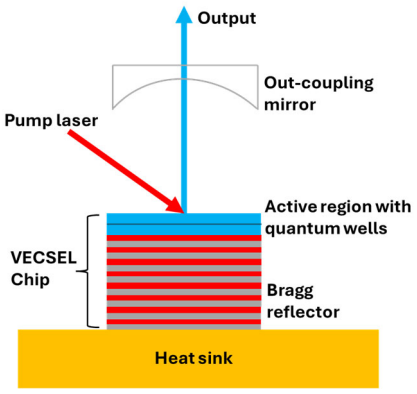

Figure 1. Schematic representation of a VECSEL and its key components.

 doi:10.20944/preprints202604.0253.v1

The utility of the VECSEL is further multiplied by its external cavity design, which facilitates intra-cavity frequency conversion. This allows the device to reach extremes of the electromagnetic spectrum:

- Ultraviolet (244 nm): Achieved through higher-harmonic generation [11].
- Terahertz (THz): Generated via difference-frequency generation [12,13]. Table 1 summarizes the material systems, the spectral ranges and the key advantages of VECSELs.

Table 1. Summary of VECSEL material systems, spectral ranges, and key advantages.

Material system	Typical range	Key advantage	Ref
GaAs / GaN	Visible to Near-IR	High power and efficiency	[14,15]
InP / GaSb	Mid-IR	Gas sensing/Spectroscopy	[16,17]
Quantum Dots	654 nm–1.3 μm	Broad tunability	[18,19]

Ultimately, the synergy of semiconductor band-gap engineering and nonlinear optics allows VECSELs to span almost any desired wavelength for scientific or industrial use, combining the beam quality of solid-state lasers with the flexibility of semiconductors.

2.1. Thermal Management in VECSELs

After fabrication, certain VECSEL configurations require a bonding process to attach the chip to a high-thermal-conductivity mount connected to a cooling circuit. Thermal management is typically achieved using a copper heat sink and a water-cooling system to ensure efficient heat dissipation [7]. Thermal management is a critical factor in VECSEL performance, as heat buildup limits output power due to quantum defect and non-radiative losses, particularly Auger recombination [20–22].

Effective heat dissipation strategies, such as optimized pump-beam profiles and advanced cooling techniques, have been extensively studied to enhance efficiency.

Two primary heat-spreading approaches exist: Intra-Cavity Heat Spreading (ICHS) and Extra-Cavity Heat Spreading (ECHS). ICHS integrates a transparent heat spreader within the cavity, ensuring efficient cooling but potentially introducing optical losses and spectral artifacts [23,24]. ECHS, in contrast, involves flip-chip bonding the gain chip to a heat spreader, often made of Chemical-Vapor-Deposition (CVD) diamond, enabling superior thermal dissipation [25].

While ECHS is highly effective for GaAs-based VECSELs, material systems with lower thermal conductivity may require trade-offs between DBR thickness and reflectivity.

Ultimately, optimizing thermal resistance and heat flux is crucial for high-power operation, influencing factors such as wavelength stability and loss mechanisms. Different configurations, including alternative pumping schemes and heat-spreader designs, continue to evolve to maximize VECSEL efficiency.

2.2. Dual- Wavelength and Dual-Frequency VECSEL Architectures

Dual-wavelength operation in VECSELs refers to the ability of the laser to emit light simultaneously at two distinctly different optical wavelengths, typically separated by a few nanometers. This phenomenon is desirable for various applications, such as spectroscopy, terahertz generation, and optical sensing. One of the key mechanisms enabling this behavior is Spectral Hole Burning (SHB). SHB occurs when one laser mode saturates the gain medium at a specific wavelength, effectively creating a 'hole' in the gain spectrum. This local depletion of gain allows a second mode, at a different wavelength, to reach the threshold and lase as well [26,27]. This process leads to a non-uniform carrier distribution in the quantum well, enabling dual-mode operation. The quantum wells themselves provide a broad gain spectrum, supporting dual-mode lasing under conditions such as SHB or external cavity feedback, due to their tunability and high saturation intensity.

 doi:10.20944/preprints202604.0253.v1

Another approach involves two independent VECSEL chips [28,29] each operating at different frequencies, either sharing an external cavity or operating independently, with the beams combined via nonlinear optical processes or beam combiners.

Dual-Frequency VECSEL emission involves designing spatially distinct cavity modes within the same VECSEL structure, using adjusted cavity geometry or birefringent elements to ensure the frequencies stay within the quantum well's gain bandwidth. Dual-frequency lasers emit two closely spaced optical frequencies, typically within the same wavelength band, separated by MHz to GHz. This configuration is often used in applications such as radio-frequency (RF) signal generation, coherent detection, or high-resolution interferometry. Intra-cavity birefringent elements, like YVO_4 crystals, introduce birefringence, splitting polarization or frequency states, with the separation between frequencies determined by the crystal's birefringence and orientation [30,31]. Additionally, intra-cavity interference elements, such as etalons or birefringent filters, selectively stabilize two discrete frequencies while suppressing others.

2.3. Comparison of Dual-Frequency VECSEL and Dual-Wavelength VECSEL Architectures

2.3.1. Performance Metrics Based on Application Requirements

In this paper we will be comparing three advanced architectures for dual-wavelength and dual-frequency VECSELs, each tailored to different application domains. The first category includes Z-cavity, V-cavity, and F-cavity designs engineered for THz generation via spatial mode control, grating feedback, and spatial hole burning, enabling stable dual-wavelength output and tunable THz difference frequencies. The second architecture comprises dual-chip systems in serial, T-shaped, or external enhancement cavity configurations, optimized for nonlinear frequency conversion processes like Difference-Frequency-Generation (DFG), Second-Harmonic-Generation (SHG), and Sum-Frequency- Generation (SFG), offering high intracavity powers and broader wavelength separations for THz and visible light generation. The third architecture features dual-frequency VECSELs (DF-VECSELs) using birefringent crystals to generate two orthogonally polarized modes with closely spaced frequencies for microwave photonics, atomic clocks, and fiber sensing. While the designs differ in physical structure and mechanism, they are evaluated against a common set of performance criteria tied to their intended applications.

2.3.2. Performance and Design Considerations

These performances and criteria are listed below:

1. Output power / intracavity power: Higher power enables stronger THz output, more efficient DFG/SHG/SFG, and sufficient signal for sensing or clock interrogation (critical for THz communication, spectroscopy, and fiber sensing).
2. Spectral linewidth: Narrow linewidths (<1 MHz or sub-100 kHz) ensure coherence and spectral purity, crucial for time-domain spectroscopy, atomic clocks, and coherent communication.
3. Frequency / Beat-note tunability: Tunability over GHz-THz ranges or specific RF bands (e.g., 9.192 GHz for Cs clocks) supports multi-application flexibility from quantum metrology to THz imaging.
4. Wavelength separation: Adjustable dual-wavelength spacing allows control over difference frequencies in DFG-based THz generation and facilitates access to a wider nonlinear optical spectrum.
5. Polarization control: Orthogonal or tunable polarization is required for efficient nonlinear interactions (type-I or type-II phase matching) and stable beat-note generation in DF-VECSELs.
6. Relative Intensity Noise (RIN) and Frequency Noise: Low RIN and minimal frequency drift ensure stable operation in microwave photonics and CPT-based clocks.
7. Thermal and long-term stability: Effective heat management and stable frequency output (e.g., $<10^{-14}$ drift over 10,000 s) are vital for cycle systems, field sensors, and clocks.

 doi:10.20944/preprints202604.0253.v1

8. Nonlinear conversion efficiency: High SHG/SFG/DFG efficiency directly determines whether the optical output meets the power and spectral purity requirements of practical THz or visible-light applications.
9. Compactness and integration potential: Especially relevant for atomic clocks and portable sensing platforms, compact VECSEL modules must be scalable and field-deployable.

Each design prioritizes these criteria differently, based on the demands of its target application, ranging from high-power, tunable THz generation to ultra-stable dual-frequency sources for timing, sensing, and quantum technologies.

3. Dual-Wavelength VECSEL Architectures

This section explores the various methods used to simultaneous emission at two distinct wavelengths from a VECSEL system.

3.1. Dual-Wavelength VECSEL Realization Using External Feedback and Multi-Folded Cavities (Optical Design)

The two color VECSEL presented in this section is designed for THz generation, which has a wide variety of applications such as time domain spectroscopy [32], medical imaging [33], industrial inspection [34], and achieve ultrafast wireless communication [35]. This approach is used due to its key advantages, including the ability to deliver high optical power, maintain a narrow spectral linewidth for high spectral purity, and offer continuous wavelength tunability through adjustments to the cavity or filtering elements [36]. A wide wavelength tunability in VECSELs using external feedback from a diffraction grating was demonstrated in [36].

Continuous tuning of a single-color VECSEL over 10 nm and controlled frequency difference in dual-wavelength emission from 300 GHz to 3.5 THz was achieved. The experimental setup utilized a Z-shaped cavity geometry consisting of a curved and a flat high-reflectivity (HR) mirror, along with a 1% output coupler (OC). A Brewster window (BW) ensured linear polarization. The cavity was folded around the OC, allowing one beam to serve as the laser's output while the other was directed to a diffraction grating (G) [36]. For two-color emission, a dual-feedback configuration incorporated two additional mirrors to form two Z-cavities, enabling independent control of both lasing wavelengths (Figure 2). The system produced 3 W of output power with high spectral purity and stability, demonstrating potential for applications such as terahertz wave generation. Using a Z-cavity in this setup contributed to improved beam quality, mode stability, power scalability, and overall performance, making it suitable for high-power, tunable laser applications.

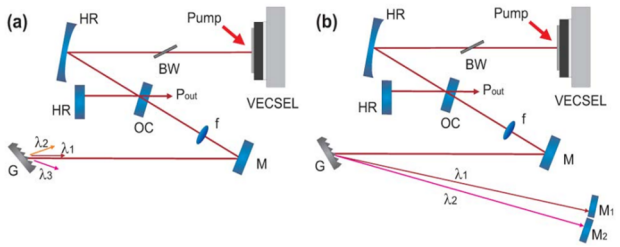

Figure 2. Figures showing the Schematics of the z-shaped cavities geometry. Reproduced with permission from [36], copyright 2012, OPTICA.

A novel multi-folded cavity design to address mode competition and enhance stability was proposed in [37]. While earlier studies [36] relied on external enhancement cavities and precise phase-locking techniques to ensure frequency stability and efficient THz generation, [37] simplified the system by using a cavity design that induced spatial interference, reducing mode competition and stabilizing dual-wavelength emission with minimal complexity. The study presented a dual-wavelength VECSEL that generated 2.6 W of continuous-wave radiation at 1015 nm, with a terahertz

 doi:10.20944/preprints202604.0253.v1

difference frequency of 1 THz between the two wavelengths. The multi-folded cavity design reduced mode competition and improved stability by creating spatial interference patterns within the gain medium. This design led to more stable dual-wavelength emission, with minimal amplitude noise and enhanced output power compared to previous approaches. The setup used a fused silica etalon to achieve a 1-THz free spectral range and demonstrated the ability to adjust the difference frequency by tilting the etalon. Dual-wavelength operation was achieved with stable output power, and the F-cavity configuration proved more effective than the V-cavity by minimizing mode competition and ensuring steady performance across a range of pump powers. The results highlighted the utility of the F-cavity design for applications requiring consistent, high-power dual-wavelength emission (Figure 3).

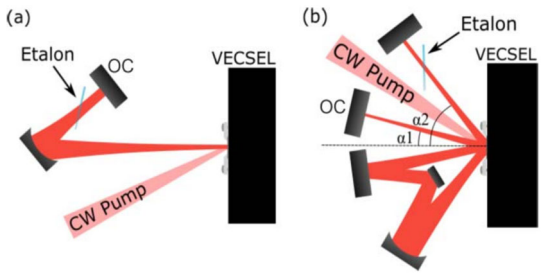

Figure 3. Schematics of the VECSEL configuration: (a) The V-cavity on the left features a single, perpendic-ular incidence on the VECSEL chip. (b) The F-cavity on the right includes two reflections over the VECSEL chip at angles α_1 and α_2 Reproduced with permission from [37], copyright 2017, IEEE.

Table 2 summarizes the findings and compares the V-cavity, F-cavity and Z-cavity setups.

Table 2. Comparison between V-Cavity, F-cavity and Z- cavity.

Aspect	V-Cavity	F-Cavity	Z-Cavity
Output Power	- Maximum: 1.3 W - Dual-wavelength: ~1 W	- Maximum: >3 W - Dual-wavelength: 2.6 W	- Maximum: 3 W - Dual-wavelength: not explicitly stated
Mode Competition	- Strong mode competition observed - Significant anticorrelated amplitude noise	- Weak mode competition observed - Minimal amplitude noise	- Moderate mode competition - Controlled dual-mode emission via etalon tuning and gain shaping
Stability	- Unstable dual wavelength operation - Sensitive to pump fluctuations	- Stable over a wide pump power range - Tolerant to pump fluctuations	- Good thermal and spectral stability - <15% intensity variation across 300 GHz to 3.5 THz tuning
Interference Pattern	- None (single reflection from VECSEL chip) - Perfect spectral mode overlap	- Strong interference due to multiple bounces - Partial decoupling of gain contributions (~45% overlap)	- Not explicitly stated
Effective Gain	- Lower effective gain	- Higher effective gain from multi-bounce design	- Enhanced effective gain via 300 W intracavity power - Uses 90% reflective grating feedback

 doi:10.20944/preprints202604.0253.v1

Pump Power Sensitivity	- Narrow operational range for dual-wavelength	- Wide operational range with gradual intensity change	- Not explicitly quantified—Stable up to 25 W pump power - No thermal roll-over observed
Localized Field Intensity	- Standard Gaussian distribution	- Enhanced localized intensities due to interference	- Very high intracavity intensity (~300 W) - Suitable for nonlinear effects like THz DFG
Tuning Capability	- Limited - Can adjust via etalon tilt or pump power changes	- Broader tuning via mirror angles and etalons	- Wide spectral tuning: 10+ nm (Littrow grating rotation) - Dual-mode difference frequency tuning: 300 GHz to 3.5 THz
Applications	- Less suited for stable dual-wavelength emission	- Ideal for stable, high-power dual-wavelength operation	- Suitable for THz generation, spectroscopy, nonlinear optics - Dual-mode emission well controlled
Intensity Product Stability	- Strong fluctuations	- Stable (1/e variance < 0.5%)	- Not explicitly stated

The study in [26] demonstrated improvements in stability and simplicity for dual-wavelength VECSEL-based THz generation by employing internal cavity design strategies. The VECSEL system, generated continuous-wave (CW) THz radiation at 1.9 THz via difference frequency generation (DFG). Dual-frequency operation was achieved within the VECSEL cavity, where mode competition was minimized by using multiple cavity folds and spatial hole burning (Figure 4). Hole burning on the gain chip enabled a partial spatial decoupling of the two lasing frequencies. Unlike conventional VECSELs, which exhibit negligible spectral hole burning in CW operation, the double-folded cavity (F-cavity) design played a crucial role in reducing mode competition. By folding the circulating laser field twice at different angles (10° and 48°), the overlap of the two wavelengths in the gain medium was minimized, leading to spatial separation of their gain regions [26].

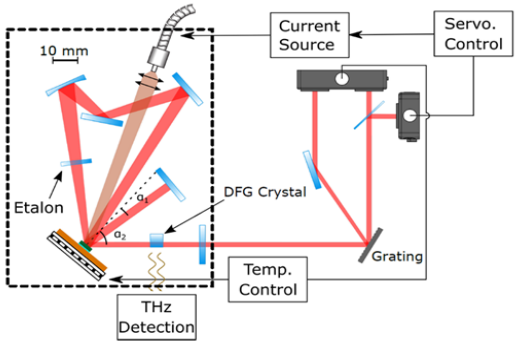

Figure 4. The described F-cavity, used to minimize mode competition between the two emitted wavelengths. The laser beam is folded multiple times onto the gain chip at different angles. Reproduced with permission from [26] copyright 2020, SPIE.

Temperature-based feedback and active stabilization were employed to reduce noise and maintain a stable power ratio between the two wavelengths, enhancing THz stability. The system achieved 2.1 mW of THz output with reduced intensity noise (from 8% to below 2%) and showed

 doi:10.20944/preprints202604.0253.v1

strong potential for stable, high-power THz generation, suitable for spectroscopy and sensing applications. The calculated quantum efficiency of the system was approximately 0.0148%.

A widely used method for selecting dual wavelengths involves the insertion of frequency-selective elements into the external cavity. While standard quartz birefringent filters (BRFs) are common, In [38] it was demonstrated that material selection is critical for achieving high-performance dual-wavelength operation. By utilizing high-birefringence KTP instead of quartz, they achieved sub-THz to tens of THz wavelength spacing with a filter thickness of only a few millimeters. This setup achieved a high linearly polarized output power of 3.53 W and was successfully integrated with an intracavity optical parametric oscillator (OPO). This configuration enabled efficient conversion to the mid-infrared (mid-IR) region, yielding 153 mW of idler wave output while avoiding the self-pulsing effects typical of external OPO setups. Furthermore, under strong depletion, the system exhibited a unique 'hole burning' effect, resulting in a multi-wavelength output with up to five equally spaced frequency peaks. Such synchronized sources are highly promising for gas detection, THz technology, and the generation of high-bandwidth mode-locked pulses.

Building on these dual-wavelength engineering approaches, Tsaoussis et al. demonstrated a fundamentally different architecture that extends the concept into the ultrafast regime. Their design employs two independent V-cavities sharing a single gain chip, with each cavity lasing at a different angle and therefore supporting its own mode-locked pulse train. Despite their spatial separation, the two pulse trains remain mutually coherent and carve distinct kinetic holes in the carrier distribution, a behavior confirmed through full Maxwell-semiconductor-Bloch simulations. Experimentally, the system produced stable ~600 fs pulses at slightly different GHz repetition rates with minimal crosstalk, highlighting excellent isolation between the two lasing channels. This dual-comb-like configuration enables compact, coherent multi-source operation, offering strong potential for applications such as dual-comb spectroscopy and time-resolved pump-probe measurements [39].

3.2. Multi-Component Quantum Well Engineering (Internal Design)

The most integrated approach to dual-wavelength emission involves the direct engineering of the semiconductor active region. By growing multiple groups of quantum wells (QWs) with different bandgaps within a single gain chip, researchers can achieve multi-wavelength operation without complex external optics.

- Broad Spectral Spacing: Zhang et al. [40] demonstrated a single-chip VECSEL using two types of InGaAs QWs to produce a stable 45 nm spacing (967 nm and 1013 nm). This was achieved by strategically positioning the wells within the standing-wave field to balance gain and compensate for thermal drift.
- Self-Induced Pulsing and Dynamics: Building on this architecture, Li et al. [41] utilized a similar single-chip design with QW groups emitting at 975 nm and 978 nm. A unique aspect of this implementation is the use of internal QW absorption dynamics. At specific pump powers, one QW group acts as a dynamic absorber and modulator, triggering self-induced nanosecond pulses (~9 ns) at a 54 MHz repetition rate without the need for an external SESAM. As pump power increases, the system transitions into a stable dual-wavelength CW mode, demonstrating the versatility of QW engineering for both pulsed and continuous-wave applications in optical computing.
- Further advancing the single-chip architecture [40] is the development of a VECSEL capable of switching between 955 nm and 997 nm. By integrating two sets of InGaAs quantum wells (gain peaks at 930 nm and 980 nm) and matching them with a dual-mode Fabry-Perot cavity, the researchers utilized internal self-heating to shift the gain peaks. By simply varying the pump power, the laser can be toggled between single-wavelength and dual-wavelength modes, achieving a simultaneous output of 250 mW.
- The 42 nm wavelength separation is specifically designed for Difference Frequency Generation (DFG) to produce Terahertz radiation. This compact single-chip approach is presented as a more effective alternative to complex multi-chip setups, providing the high beam quality and power

 doi:10.20944/preprints202604.0253.v1

required for specialized applications in astronomy, pharmaceutical analysis (measuring tablet porosity), and high-speed communication.

3.3. Dual-Wavelength VECSEL Realization Using External Feedback and Multi-Folded Cavities (Optical Design)

While the previous sections discuss external cavity manipulation, another robust approach involves engineering the gain profile directly within a single VECSEL cavity. Recent studies in [42] a compact, stable, and highly tunable continuous-wave (CW) Terahertz (THz) generation system operating at the advantageous 1064 nm wavelength was demonstrated. This wavelength is particularly significant as it addresses the scarcity of high-efficiency components compared to the more common 1550 nm telecommunications band.

The implementation of this system utilizes a novel Dual-Frequency VECSEL (DF-VECSEL) that leverages modal gain selection via internal metallic masks and a cylindrical thermal gradient. This combination robustly stabilizes two distinct transverse modes, enabling coherent dual-frequency operation. Key performance metrics include:

- Tuning Range: A beat frequency range of 50–900 GHz, controlled primarily by pump power.
- Stability: A beat signal frequency noise four orders of magnitude lower than the optical noise.
- Application: By combining this stable source with a 1064 nm-designed plasmonic photomixer, the overall optical-to-THz conversion efficiency is significantly improved, paving the way for more accessible and portable THz applications [42].

3.4. Dual-Wavelength Realization Using Two VECSEL Chips

For applications requiring maximum power or independent control of each wavelength, a two-chip configuration is preferred.

3.4.1. Thermal Management and Frequency Doubling in Two-Chip Cavities

Beyond dual-wavelength emission, the two-chip configuration is a powerful architecture for scaling output power in visible light generation through nonlinear frequency conversion. A notable implementation by [43] utilizes two identical VECSEL chips in a bow-tie ring cavity to generate high-power yellow emission at 589 nm.

The implementation highlights several key advantages of the multi-chip approach:

- Thermal Load Distribution: By using two chips instead of one, the thermal load is distributed, allowing for higher intracavity power without reaching the thermal rollover point.
- Nonlinear Efficiency: The high intracavity power at the fundamental wavelength (1178 nm) enables efficient Second-Harmonic Generation (SHG) using an LBO crystal.
- Performance: The system achieved a maximum average yellow output power of 264 mW with a microsecond-pulsed format, specifically designed for sodium laser guide-star applications.

Wavelength tuning from 576 nm to 602 nm was facilitated by an intracavity birefringent filter (BRF), which also enforced the polarization required for efficient type-I non-critical phase matching. This work demonstrates that the two-chip architecture is not only robust for frequency separation but is essential for high-brightness applications that require efficient nonlinear conversion.

3.4.2. Dual-Chip Architectures for High-Power THz Generation via DFG

In [19], Guoyu et al. presented a different approach for terahertz (THz) generation compared to the previous case [26] using two-Chip VECSEL configuration allowing for higher intracavity powers and improved THz output compared to single-chip configurations. The key differences are the use of:

1. Frequency conversion and output power: Intracavity frequency conversion using a periodically poled lithium niobate (PPLN) crystal for DFG, but the focus is on achieving THz output in a

 doi:10.20944/preprints202604.0253.v1

type-I frequency conversion scheme at room temperature. It demonstrates THz output powers up to 650 μW, with intracavity powers exceeding 820 W, which is more focused on power scaling rather than the stability and noise reduction aspects highlighted previously.

2. Wavelength tunability: tunability of the generated THz output with a 3.5 nm wavelength separation (around 1.025 THz), providing a broader application scope for tunable THz sources.

In [44], the study also focused on dual wavelength VECSELs for THz generation via difference frequency generation (DFG), employing phase-locking techniques to achieve narrow-linewidth THz radiation, with applications in precision spectroscopy and radio astronomy. However, in this case, the study incorporated an external enhancement cavity with a buildup cavity for phase-locking. Additionally, advanced thermal management and stabilization techniques were employed, contributing to higher power scaling and improved frequency stability. The VECSELs were optically pumped by an 808 nm fiber-coupled diode laser, with feedback elements like a birefringent filter and etalon ensuring single-frequency operation. THz radiation was produced via difference frequency generation (DFG) in an external tilted periodically poled lithium niobate (TPPLN) crystal. Polarization alignment of the laser beams is achieved using a thin-film polarizer and multi-order waveplate.

The buildup cavity, a ring cavity with flat and curved mirrors, locks the VECSELs through a feedback control system, achieving intracavity powers in the hundreds of watts and generating over 110 μW of THz output (Figure 5). The system ensured excellent frequency stability, with phase-locking to the external buildup cavity using the Hänsch-Couillaud technique and further stabilization of one VECSEL to a zerodur reference cavity, minimizing drift to less than 12 MHz. Linewidth measurements, conducted via Michelson interferometer and heterodyne detection, confirm sub-100 kHz linewidth.

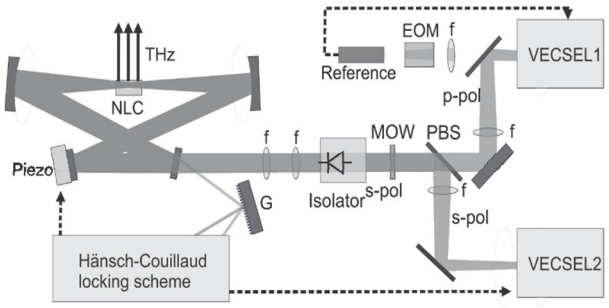

Figure 5. Layout of the THz source in [43]- The output of two single frequency VECSELs is combined using a polarizing beam splitter (PBS). A multi-order-waveplate (MOW) rotates both beams to the same polarization state. The combined beam is guided through an optical isolator and mode matching lenses (f). To lock the beams to the external resonator containing a nonlinear PPLN crystal, a grating (G) is employed to spatially separate both wavelength components reflected from the cavity. The Hänsch-Couillaud scheme is used to provide error signals for the locking. One of the VECSELs is frequency stabilized to a reference cavity using an electro-optical-modulator (EOM) and the Pound Drever Hall locking technique. Reproduced with permission from [42] copyright 2019, SPIE.

In VECSELs, dual-wavelength operation for difference-frequency generation (DFG) and sum-frequency generation (SFG) is typically achieved by incorporating a Fabry-Perot etalon within the cavity [28,29]. However, this approach limits the wavelength separation to just a few nanometers due to the gain bandwidth constraints of a single VECSEL chip. An alternative method was proposed by Hessenius et al. [45] who utilize a T-cavity configuration with two VECSEL chips emitting at different wavelengths. Lukowski et al. have achieved 300 W of intracavity power for Difference Frequency Generation (DFG) in such a two-chip cavity [46]. However, since the two wavelengths in this setup are orthogonally polarized, it is only suitable for type-II frequency conversion.

 doi:10.20944/preprints202604.0253.v1

In [47], the realized setup enabled linearly polarized dual-wavelength emission with up to 640 W intracavity power, tunable through cavity angle adjustments. Additionally, it facilitated type-I second harmonic generation (SHG) and sum-frequency generation (SFG) using a $LiNbO_3$ crystal. A V-shaped single-chip cavity was initially employed to investigate the impact of cavity angle on the emission wavelength of a VECSEL chip. It was observed that adjusting the cavity angle induced a blue shift in the emission wavelength. Building on this, a dual-chip VECSEL configuration was designed with cavity angles of 45° and 20°, achieving a 10-nm wavelength spacing, which is difficult to obtain in a single-chip system. This arrangement produced dual-wavelength emission at 1 μm with up to 640 W intracavity power. The two wavelengths exhibited antiphase behavior, suggesting partial gain overlap between the two chips.

In this context, 'serially' refers to the sequential arrangement of two distinct gain chips along the optical path within the same laser cavity. Light emitted by the first gain chip interacts with the second, allowing efficient utilization of both gain media within a single cavity. This configuration maintains high intracavity power while enabling dual-wavelength emission. The system further supports intracavity frequency conversion, demonstrating SHG and SFG, with the converted frequencies presented in the inset spectrum of Figure 6 (cyan line).

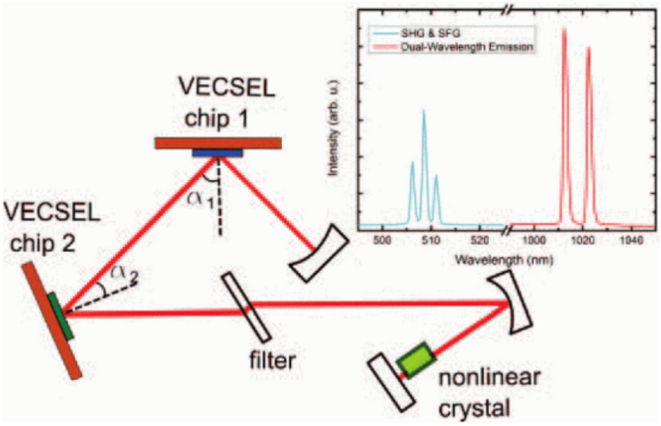

Figure 6. Schematic of the two-chip VECSEL setup. Inset: emission spectrum showing the dual-wavelength output (red) alongside the generated second-harmonic and sum-frequency signals (cyan) [47]. Reproduced with permission from [47] copyright 2016, IEEE.

A two-color collinear vertical external-cavity surface-emitting laser (VECSEL) was developed to generate widely tunable sum-frequency signals in the visible range [47,48]. By optimizing the laser cavity and nonlinear conversion process, the sum-frequency generation (SFG) was achieved with broad tunability and high power stability. This setup enabled efficient nonlinear frequency conversion and has potential applications in precision spectroscopy and imaging. The work involved designing the laser architecture, optimizing wavelength tuning, and enhancing output stability, contributing to the advancement of compact, tunable light sources.

A compact and versatile cavity design for dual-wavelength VECSELs, integrating serially connected gain chips within a single cavity was presented in [47], which facilitated type-I second harmonic generation (SHG) and sum-frequency generation (SFG) using a $LiNbO_3$ crystal.

A greater flexibility beyond 10 nm was achieved in [48] instead of cavity angle tuning. This system employed Bragg reflectors (BRFs) and chip selection to control wavelength separation. The resonator included a Brewster-angled BRF, ensuring p-polarization for efficient type-I frequency conversion. Enhanced thermal management is achieved through diamond heat spreaders and a water-cooled copper heat sink, enabling stable operation at over 600 W intracavity power.

Simultaneously pumping both chips broadened the gain bandwidth compared to single-chip operation. Initially, a 1-mm BRF resulted in minimal gain overlap, but replacing it with a 10-mm BRF (matching the 10 nm separation) enabled stable dual-wavelength emission. Similar to [47], antiphase fluctuations were observed, confirming partial gain overlap. The system successfully demonstrated

 doi:10.20944/preprints202604.0253.v1

SHG and SFG using a periodically poled $LiNbO_3$ (PPLN) crystal and explored difference-frequency generation (DFG) for potential THz emission around 3 THz. The set-up is shown in Figure 7.

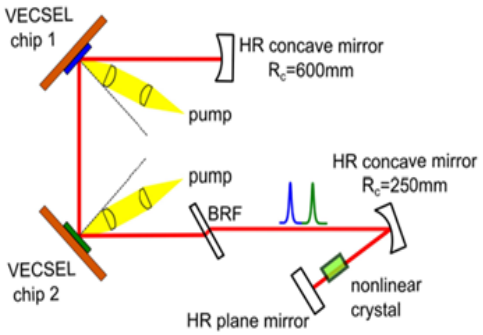

Figure 7. showing the drawing of the set-up in [48] with two chips, HR mirrors, and a tunable BRF for wavelength selection. Reproduced with permission from [48] copyright 2016, IEEE.

Table 3 summarizes the different Dual-Wavelength VECSEL Architectures.

Table 3. Summary of Dual-Wavelength VECSEL architectures.

Architecture	Key design	Applications	Notable Performance	Ref
External Feedback & Multi-folded Cavities	Use of Z-shaped or F-shaped cavities with diffraction gratings or etalons.	THz generation, medical imaging, spectroscopy.	High spectral purity, F-cavity design minimizes mode competition and noise (below 2%).	[26,36,37]
Intracavity Material Selection	Use of high-birefringence KTP filters instead of quartz.	Mid-IR conversion via OPO, gas detection.	3.53 W power, achieves sub-THz to tens of THz spacing with thin filters.	[38]
Quantum Well (QW) Engineering	Integration of multiple QW groups with different bandgaps on a single chip.	Compact THz sources, optical computing.	42–45 nm wavelength spacing, can toggle between CW and self-induced pulsing.	[40,41]
Intracavity Modal Engineering	Use of internal metallic masks and cylindrical thermal gradients.	280 GHz radiation, portable THz apps.	Stabilizes transverse modes, beat frequency tuning (50–900 GHz) via pump power.	[42]
Two-Chip Configuration (General/SHG)	Serial arrangement of two chips in a bow-tie or T-cavity.	Visible light (yellow 589 nm), sodium guide-stars.	Distributes thermal load, high intracavity power for efficient frequency doubling (SHG).	[43,45,46]
Two-Chip DFG/SFG Scaling	Dual chips with phase-locking or specific cavity angles (V/T-shapes).	High-power THz generation, radio astronomy.	Intracavity power >800 W, phase-locking reduces drift to <12 MHz, sub-100 kHz linewidth.	[28,44,47,48]
Quantum Well (QW) Engineering	Integration of multiple QW groups with different bandgaps on a single chip.	Compact THz sources, optical computing.	42–45 nm wavelength spacing, can toggle between CW and self-induced pulsing.	[40,41]

 doi:10.20944/preprints202604.0253.v1

Intracavity Modal Engineering	Use of internal metallic masks and cylindrical thermal gradients.	280 GHz radiation, portable THz apps.	Stabilizes transverse modes, beat frequency tuning (50–900 GHz) via pump power.	[42]
Two-Chip Configuration (General/SHG)	Serial arrangement of two chips in a bow-tie or T-cavity.	Visible light (yellow 589 nm), sodium guide-stars.	Distributes thermal load, high intracavity power for efficient frequency doubling (SHG).	[43,45,46]
Two-Chip DFG/SFG Scaling	Dual chips with phase-locking or specific cavity angles (V/T-shapes).	High-power THz generation, radio astronomy.	Intracavity power >800 W, phase-locking reduces drift to <12 MHz, sub-100 kHz linewidth.	[28,44,47,48]
Quantum Well (QW) Engineering	Integration of multiple QW groups with different bandgaps on a single chip.	Compact THz sources, optical computing.	42-45 nm wavelength spacing, can toggle between CW and self-induced pulsing.	[40,41]
Intracavity Modal Engineering	Use of internal metallic masks and cylindrical thermal gradients.	280 GHz radiation, portable THz apps.	Stabilizes transverse modes, beat frequency tuning (50-900 GHz) via pump power.	[42]
Two-Chip Configuration (General/SHG)	Serial arrangement of two chips in a bow-tie or T-cavity.	Visible light (yellow 589 nm), sodium guide-stars.	Distributes thermal load, high intracavity power for efficient frequency doubling (SHG).	[43,45], [45]
Two-Chip DFG/SFG Scaling	Dual chips with phase-locking or specific cavity angles (V/T-shapes).	High-power THz generation, radio astronomy.	Intracavity power >800 W, phase-locking reduces drift to <12 MHz, sub-100 kHz linewidth.	[28,44,47,48]

4. Dual-Frequency VECSEL Architectures

Dual-frequency VECSELs (DF-VECSELs) offer a highly tunable solution for generating optically carried single-sideband RF signals with exceptional spectral purity. Their advantage lies in laser class-A dynamics, where the photon lifetime inside the cavity far exceeds the excited carrier lifetime, effectively suppressing common-mode noise. As a result, the beat-note remains highly stable and can be more easily phase-locked to an external reference than independent lasers [49]. This makes DF-VECSELs particularly valuable for applications in microwave photonics, including optical telecommunications, radar, and LiDAR [50], and other applications. Additionally, because both oscillating polarized modes share the same cavity, the frequency difference between them can be adjusted by tuning the intra-cavity phase anisotropy.

The stability of dual-frequency operation in VECSELs is strongly influenced by the nonlinear coupling constant (C), which governs the interaction between the two lasing modes. Studies on QW-based VECSELs have shown that (C) remains stable (~0.84) across a wide range of frequency separations (45 GHz to 1.35 THz) [51], ensuring correlated phase and intensity fluctuations between the modes. While some designs achieved stable operation without spatially separating the modes [51]. Other studies introduced a 1 mm spatial separation within the cavity to mitigate strong coupling effects [52]. Both approaches confirm that as long as C remains below unity as discussed in [53], dual-frequency operation remains stable, making VECSELs a robust platform for tunable dual-wavelength emission.

DF-VECSEL operation was achieved at different wavelengths and will be discussed below.

 doi:10.20944/preprints202604.0253.v1

4.1. DF-VECSEL at 1 Micrometer

To achieve DF emission at 1 μm, the described setup in [54] featured a half-VCSEL gain chip at 1 μm, a high-reflectivity concave mirror, and a birefringent crystal to spatially separate polarization modes, reducing coupling and enabling stable dual-frequency oscillation. An etalon was used to enforce single-mode operation, and an additional birefringent crystal allowed frequency tuning. The beat-note frequency was continuously tunable from a few MHz to 3.66 GHz, with a spectral linewidth of 4 kHz. This approach presented a significant advancement in the development of low-noise dual-frequency lasers, particularly for applications in high-precision metrology, microwave photonics, and coherent optical communication.

4.2. DF-VECSEL at 852 Nanometer

The first demonstration of a dual-frequency VECSEL at 852 nm was reported in [55], utilizing a birefringent YVO_4 plate to induce dual-frequency, dual-polarization emission for coherent population trapping (CPT) of cesium atoms. The cavity configuration was the similar to the cavity described previously in [54]. This work established the fundamental cavity design for DF-VECSELs for (CPT) of cesium atoms, which remained unchanged in later developments. However, the active region and fabrication process underwent significant optimization in subsequent research. The improvements included modifications to the semiconductor structure, quantum well composition, and growth techniques, enhancing output power, efficiency, and stability. This laser operated with a pump power density of 7.96 kW/cm⊚and a quantum efficiency of 6.33%, while later advancements focused on further optimizing these parameters. These refinements were crucial in improving performance for CPT-based atomic clocks, reducing noise, and ensuring compatibility with high-precision timing applications. In [30], the DF-VECSEL was optimized for coherent population trapping (CPT) of cesium atoms. The VECSEL structure included a 30 λ/4-thick active region with seven 8-nm GaAs quantum wells, supported by a high-reflectivity bottom DBR and a GaAs substrate (Figure 8).

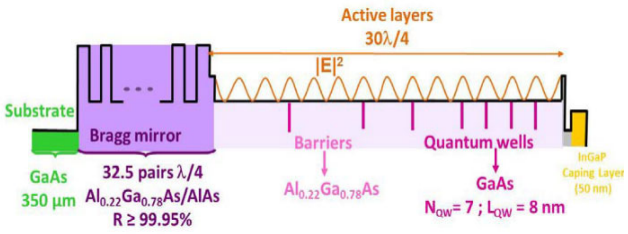

Figure 8. Figure showing the semiconductor structure design [30]. Reproduced with permission from [30] copyright 2013, SPIE.

The pump source was a 1.6 W laser diode at 670 nm, focused through an aspherical lens into a 100 μm multimode fiber. The compact cavity was 10 mm long, with a free spectral range of 12 GHz, and the output coupler was mounted on a piezoelectric transducer for cavity tuning. Dual-frequency emission was achieved using a birefringent YVO_4 plate, which created two cross-polarized modes with distinct cavity lengths. Under a pump power of 1 W at 670 nm, the laser generated 26 mW at 852.1 nm. The frequency difference between the two modes was approximately 3 GHz and could be tuned by ±1 GHz by adjusting the temperature of the electro-optic crystal (MgO:SLT) (Figure 9).

 doi:10.20944/preprints202604.0253.v1

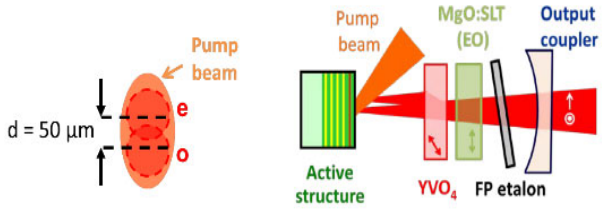

Figure 9. Experimental setup for the OP-VECSEL (right) and the laser and pump beam overlap on the chip surface (left) [30]. Reproduced with permission from [30] copyright 2013, SPIE.

Significant improvements were made to enhance DF-VECSEL performance for compact atomic clocks, by optimizing the laser architecture, refining the semiconductor gain structure, and thoroughly evaluating noise characteristics [56]. One of the key innovations was the implementation of a dual-frequency, dual-polarization emission scheme with GHz-range tunability via controlled birefringence. This feature allowed -state hyperfine transition (9.192 GHz), a crucial requirement for CPT-based atomic clocks. The active region underwent further refinement, incorporating seven 8 nm-thick GaAs quantum wells within a distributed Bragg reflector (DBR) structure, improving pump absorption and modal gain. The quantum efficiency was measured at 2.03% with a pump power density of 4.97 kW/cm^{2}, reflecting a more optimized energy conversion compared to earlier implementations. A critical aspect of this work was the comprehensive noise analysis, demonstrating that the relative intensity noise (RIN) was limited to -110 dB/Hz due to pump RIN transfer. Frequency noise measurements revealed that mechanical and thermal fluctuations influenced the linewidth, which reached 1 MHz at 1 second in locked operation. Figure 10 shows the laser stabilization experimental set-up.

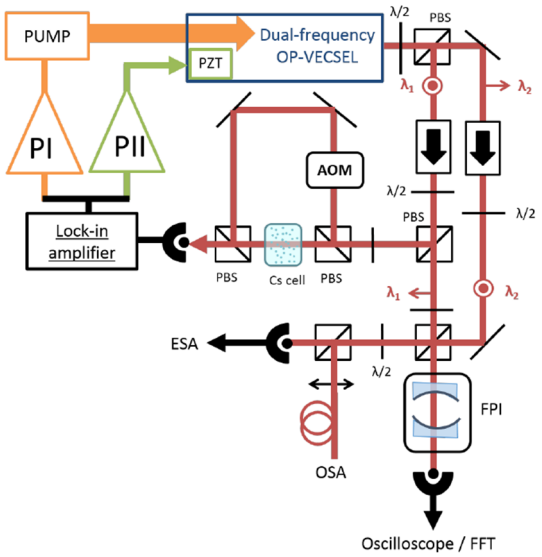

Figure 10. Laser stabilization experimental set-up. PBS: Polarizer Beam Splitter, λ 2: Half wave plate, AOM: Acoustooptic modulator, FPI: Fabry-Perot Interferometer, OSA: Optical spectrum analyzer, ESA: Electrical spectrum analyzer, PI: Proportional integrator servo, PII: Proportional with a 2-integration-stage servo, FFT: Fast Fourier Transform spectrum analyzer [56]. Reproduced with permission from [56]copyright 2015, SPIE.

Mode correlation studies have demonstrated strong coupling between cross-polarized modes, leading to a reported 5 dB reduction in RIN at 100 kHz. Beatnote linewidth measurements of dual-frequency VECSELs have shown values around 840 kHz, with theoretical models suggesting potential improvements to 500 kHz by mitigating excess mechanical noise. These findings indicate that dual-frequency VECSELs can achieve the spectral purity and frequency stability necessary for CPT atomic clock applications. Studies have further shown that stabilizing one polarization mode to

 doi:10.20944/preprints202604.0253.v1

a Cs atomic birefringence control enables compliance with atomic clock requirements. This body of work underscores the potential of semiconductor-based solutions for miniaturized atomic clocks.

Building upon previous advancements in DF-VECSEL technology, the work in [57] introduced an active optical power stabilization setup using an acousto-optic modulator and feedback loop, achieving a 25 dB RIN reduction for dual-polarization modes and 13 dB for individual modes. A predictive model was developed, aligning well with experimental results, though minor discrepancies remain due to shot noise and detection limitations. These advancements enhanced the spectral purity and stability of DF-VECSELs, marking a significant step toward fully integrated atomic clock prototypes.

The following study [58], focused on updating the design even more, the design of a compact 10 L (10 L refers to a volume of 10 liters, which is the internal space occupied by the miniature electro-optical bench. In this case, the dimensions of the enclosure (9.5 × 25 × 43 cm) gave a total volume slightly above 10 liters) electro-optical bench for stabilizing a dual-frequency laser in cesium CPT clocks. The work was focused on improving the system to simultaneously stabilize optical power and frequency, achieving a 60 dB reduction in frequency noise (with a noise floor of 40 dBHz@/Hz) and 15 dB RIN suppression (floor: -156 dB/Hz). This system integrated miniature silica-based optics, robust bonding, and AOM-based feedback loops for enhanced power and wavelength stabilization (Figure 11). The system reached frequency stability below 10^{-14} at 10 000 s.

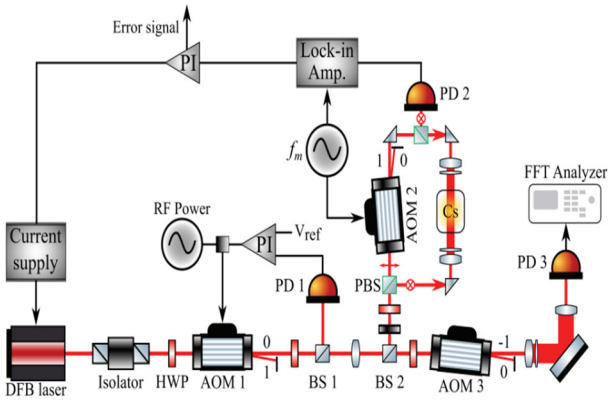

Figure 11. Intensity stabilization and frequency locking set-up. AOM: acousto-optic modulator, HWP: half-wave plate, PD: photodiode, BS: beam splitter, PBS: polarization beam splitter [58]. Reproduced with permission from [58] copyright 2022, SPIE.

4.3. DF-VECSEL at Telecom Wavelength

DF-VECSEL at telecom wavelength was realized in [31,59] for Brillouin fiber sensors. The VCSEL chip was optimized for low lasing threshold and high output power, with an active region grown on an InP substrate and a GaAs/AlGaAs DBR structure. The chip was then integrated onto a CVD diamond substrate and tuned to a resonance wavelength close to 1550 nm. The VECSEL cavity was designed with a highly reflective output mirror, and the cavity configuration is the same as previously. The cavity length was set to 9 mm, with a mode radius of 40 µm. The laser was pumped using a 980 nm diode, and output power was characterized using a polarizer, optical spectrum analyzer, and electrical spectrum analyzer. Experimental results showed that dual-frequency operation could be achieved with up to 50 mW output power. The stability of the dual-frequency emission was assessed by varying the coupling strength between cavity modes, with a stable frequency difference observed for coupling strengths ranging from 0% to 70%. The beat-note width was measured at approximately 240 kHz, with a drift of around 1 MHz/min due to mechanical vibrations.

Table 4 summarizes the dual-frequency (DF) VECSEL developments described in the text.

 doi:10.20944/preprints202604.0253.v1

Table 4. This is a table. Tables should be placed in the main text near to the first time they are cited.

Wavelength	Key features & architecture	Performance & metrics	Applications
1μm	Half-VCSEL gain chip, birefringent crystal for spatial mode separation, intra-cavity etalon.	Tunable from MHz to 3.66 GHz, linewidth: 4 kHz.	Metrology, coherent communication
852 nm	GaAs QWs, YVO_4 plate for birefringence, MgO:SLT crystal for tuning, compact 10mm cavity.	26 mW power, beat-note ~3 GHz (tunable± 1 GHz), RIN: -110 dB/Hz, beat-note linewidth: 840 kHz.	CPT-based atomic clocks (Cesium)
852 nm (Advanced)	Integration of AOM-based feedback loops, 10-liter miniature electro-optical bench.	25 dB RIN reduction, frequency stability below 10^{-14} at 10 000s, 60 dB freq. noise reduction.	Integrated atomic clock prototypes
Telecom (1550 nm)	InP-based active region, GaAs/AlGaAs DBR, CVD diamond substrate, 980 nm pump.	50 mW output power, beat-note width: 240 kHz, stable coupling up to 70%.	Brillouin fiber sensors

4.4. Noise Reduction in DF-VECSELs

Studying and optimizing noise in DF-VECSELs at different wavelengths is crucial for improving their performance and stability, particularly in high-precision applications such as atomic clocks, where low noise is vital for maintaining frequency accuracy and spectral purity. The noise characteristics of DF-VECSELs at telecom wavelengths have been extensively studied. One study demonstrated significant noise reduction by using fully in-phase correlated pumping [60]. By polarization-combining two single-mode fibered laser diodes into a single-mode fiber, perfect phase correlation was achieved, resulting in ultra-low noise levels, including relative intensity noise (RIN) below -140 dB/Hz and a 30 dB reduction in beatnote phase noise, approaching the spontaneous emission limit. Key components of the setup included:

1. Pump Lasers: Two 950 mW, 976 nm polarization-maintaining fibered diodes.
2. Polarization Combiner—Merged the two pump beams into a single-mode fiber while maintaining phase alignment.
3. Single-Mode Fiber Delivery: Ensured in-phase correlation by minimizing modal interference.
4. Beam Focusing: A telescope lens system delivered the pump light to the DF-VECSEL.

Findings underscored the importance of pump correlation for noise suppression, making DF-VECSELs more suitable for applications in microwave photonics, atomic clocks, and precision optical systems.

Simulations confirmed that increasing the pump correlation amplitude (ξ) reduces beatnote phase noise and minimizes RIN transfer. As ξ approaches 1, noise suppression is maximized, improving laser stability. An alternative approach, using a split single pump laser, provided high correlation but not full in-phase coherence, leading to partial noise reduction, though it is less effective than fully in-phase pumping [61].

As mentioned previously, the optimization of intensity and phase noise in DF-VECSELs for atomic clocks is important, as these clocks are critical for precision timing applications. However, their miniaturization is constrained by intensity and phase noise in the laser system. In [61], these limitations were addressed through a detailed analysis of noise mechanisms, pumping configurations, and active stabilization techniques. With the same configuration as mentioned previously, the DF-VECSELs operated with two orthogonally polarized modes near 852 nm, driven by a multimode pump laser. The pump power density, calculated as 10.77 kW/cm^2, provided a critical parameter for understanding how the pump energy interacts with the gain medium in the DF-VECSEL cavity, directly influencing the efficiency of gain saturation and noise behavior in the laser modes [61,62].

 doi:10.20944/preprints202604.0253.v1

The system's dynamics were characterized by pump noise correlations, which significantly impacted the intensity and phase stability of the modes. Two pumping architectures were evaluated: single-spot pumping, where modes experience high cross-saturation and anti-phase noise correlations, and dual-beam pumping, which enhanced in-phase correlations by spatially separating the pump beams. The latter architecture achieved better decoupling of pump noise, thereby reducing its transfer to the laser modes [61], Figure 12 show the two pumping architectures. Active noise suppression using feedback mechanisms was implemented to address the intensity and phase noise. Intensity noise, driven by pump fluctuations and mode cross-saturation, degraded clock stability, while phase noise in the beat-note, arising from thermal effects and phase/amplitude coupling, impacted the interrogation of cesium hyperfine transitions. To mitigate intensity noise, a feedback loop was introduced, modulating the pump current based on single-mode or total laser intensity. Dual-beam pumping combined with total-intensity feedback achieved noise reduction below -140 dB/kHz at low frequencies. Phase noise stabilization was accomplished using an Optical Phase-Locked Loop (OPLL), which adjusted intra-cavity birefringence via an electro-optic crystal. This method effectively reduced phase noise within a 100 kHz bandwidth, improving frequency stability. Experimental results demonstrated that dual-beam pumping outperforms single-spot pumping in noise suppression and stability enhancement. The addition of a lead-lag filter further improved the feedback system's performance by attenuating high-frequency noise peaks. These advancements enhance the short-term stability of CPT clocks, reinforcing the potential of DF-VECSELs for compact, high-precision atomic clock systems.

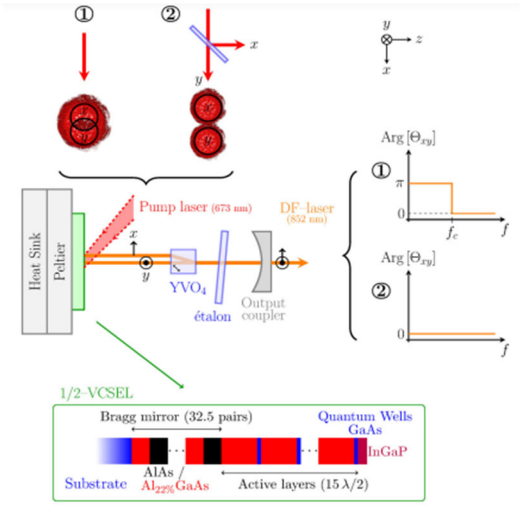

Figure 12. Dual-frequency VECSEL oscillating at 852 nm, implemented with two different pumping schemes labeled ① and ②. Scheme ① (resp. ②) leads to a large (resp. small) value of the coupling constant C between the two modes and a small (resp. large) correlation amplitude ξ between the pump noises seen by the two modes [61]. Reproduced with permission from [61] copyright 2020, OPTICA.

From [61], Table 5 summarizes the differences between dual-pump and single-pump architectures, highlighting their respective impacts on noise characteristics. At d=0 (d is the spatial separation between the two modes), the high pump power density and overlapping gain regions led to a strong coupling constant (C) and high noise correlations (~1). As d increased, reduced overlap weakened the coupling constant, decreasing noise correlation and introducing phase shifts at separations of 125–150 μm. In summary, dual-pump lasers significantly enhanced cesium clock performance by improving stability, accuracy, and efficiency. They minimize frequency and intensity fluctuations, enabling precise timekeeping and fine-tuned frequency control. By reducing phase and frequency noise, this approach ensures greater accuracy and energy efficiency, making it essential for ultra-high precision applications.

 doi:10.20944/preprints202604.0253.v1

Table 5. This is a table. Tables should be placed in the main text near to the first time they are cited.

Pumping Architecture	Single Pump Spot	Two Pump Beams
Mode overlap	Larger overlap between the two modes.	Modes are well-separated, leading to minimal overlap.
Cross-Saturation (C)	Stronger cross-saturation due to larger overlap.	Lower cross-saturation due to spatial separation.
(Correlation Amplitude, ξ)	Weaker correlation between pump noises seen by the two modes.	Stronger correlation (near perfect correlation, ξ ≈ 1).
Intensity Noise Behavior	Anti-correlated at lower frequencies, in-phase at higher frequencies.	Always in-phase at all frequencies.

Further noise analysis and mitigation in DF- VECSELs for Cesium Clocks was described in [63–65]. The noise behavior, including intensity noise in orthogonally polarized modes and phase noise in their beatnote, was analyzed using a theoretical model based on coupled rate equations. The model considered thermal effects, phase-amplitude coupling, and nonlinear interactions, offering predictive insights validated through experimental data. Pump noise, primarily influencing the intensity and phase noise, was shown to correlate with frequency-dependent effects on laser stability. Key findings revealed that noise mitigation is achievable through:

1. Balancing excitation ratios: Minimizing relative intensity noise (RIN) by equalizing the excitation ratios of the two modes.
2. Maximizing pump noise correlation (ξ): Increasing ξ to 1 significantly reduces both RIN and phase noise, particularly at low frequencies.
3. Optimizing coupling constant (C): Controlling coupling between modes minimizes noise transfer, with reduced coupling favouring anti-phase noise suppression.

Experimental results, including correlation amplitude and phase spectra, were aligned with the theoretical predictions, demonstrating the impact of nonlinear coupling and pump noise on laser dynamics. Notably, RIN exhibited class-A dynamics, with sharper spectral features as cavity length increases, driven by stronger coupling effects. This comprehensive analysis underscored the potential of DF-VECSELs for high-precision applications such as atomic clocks, radar, and RF signal generation. Table 6 summarizes key benefits of dual-pump lasers in Cesium clocks, highlighting how each benefit contributes to the system's overall performance:

Table 6. Summary of dual-pump laser advantages for Cesium clock optimization.

Benefit	Description
Enhanced frequency control	Allows precise tuning of the laser's output frequencies, ensuring the correct frequency for cesium clock operation.
Noise reduction	Helps mitigate phase and frequency noise by reducing instabilities, improving the clock's accuracy and long-term precision.
Improved efficiency	Dual-pump lasers provide better energy efficiency by balancing the power between two sources, minimizing heat generation.
Precision tuning and locking	Facilitate stable locking of the laser to an ultra-stable reference frequency, ensuring precision time measurement in cesium clocks.
Enhanced frequency control	Allows precise tuning of the laser's output frequencies, ensuring the correct frequency for cesium clock operation.
Noise reduction	Helps mitigate phase and frequency noise by reducing instabilities, improving the clock's accuracy and long-term precision.
Improved efficiency	Dual-pump lasers provide better energy efficiency by balancing the power between two sources, minimizing heat generation.
Precision tuning and locking	Facilitate stable locking of the laser to an ultra-stable reference frequency, ensuring precision time measurement in cesium clocks.

 doi:10.20944/preprints202604.0253.v1

Phase noise in the RF beatnote generated by two orthogonally polarized modes has been studied both experimentally and theoretically [66]. These studies provided insight into the coupling strength between lasing modes and its impact on phase noise. The results indicated that strong mode coupling significantly influences phase noise, particularly at higher frequencies. Adjusting this coupling allows for optimization of the spectral purity of the RF beatnote. At lower frequencies, thermal fluctuations dominate phase noise, whereas at higher frequencies, phase-intensity coupling becomes the primary noise source. An experimental setup using a 1 μm laser, pumped by a 3 W diode laser and featuring a planar-concave cavity with birefringent crystals for polarization control, demonstrated these effects. Phase noise measurements using a spectrum analyzer showed that as the coupling constant increases, phase noise transitions from thermal noise dominance to phase-intensity coupling dominance. A moderate coupling constant ($C \approx 0.35C$) provided the best balance between spectral purity and oscillation stability [53]. Negligible spontaneous emission noise and strong agreement between experimental results and theoretical models were observed in the 10 kHz–20 MHz range.

A DF-VECSEL with ultra-low intensity and beatnote phase noise operating at telecom wavelengths was also demonstrated [66,67]. This system employed two in-phase single-mode fibered laser diodes as the pump source, achieving 100% noise correlation between modes [66]. The resulting configuration led to a relative intensity noise (RIN) below −140 dB/Hz and a 30 dB reduction in beatnote phase noise, approaching the spontaneous emission limit. Residual phase noise was primarily attributed to incomplete thermal effect cancellation due to unbalanced mode pumping. The external cavity DF-VECSEL design enabled dual-mode operation with cross-polarized laser modes, achieving high spectral purity by generating a single-sideband RF signal with broad tunability and minimal noise. Compared to multimode fiber pumping, single-mode pumping with in-phase pump correlation significantly reduced intensity and phase noise. Additionally, birefringent crystals and etalons in the optimized cavity minimized gain competition, ensuring stable dual-mode oscillation. The experimental setup included two 950 mW single-mode fibered lasers at 976 nm, delivering a total power of 1.8 W. The system demonstrated tunable frequency differences up to 3 GHz, an output power of 15 mW, and low noise characteristics. From this paper we can summarize the comparison between the multimode fibered pump lasers and the single-mode fibered pump lasers for phase noise and RIN improvement in Table 7.

Table 7. Comparison between Multimode fibered pump lasers and Single-mode fibered pump lasers for DF-VECSELs.

Aspect	Multimode fibered pump lasers	Single-mode fibered pump lasers
Correlation between pumps	Low correlation between pump noises due to multimode spatial distribution.	High correlation with in-phase pump noises, reducing intensity and phase noise.
Speckle Noise	Present due to multimode interference, causing spatial incoherence and noise fluctuations.	Eliminated with single-mode fibers, removing speckle-related noise.
Relative Intensity Noise (RIN)	RIN levels between −120 dB/Hz and −130 dB/Hz in the 10 kHz to 10 MHz frequency range.	RIN levels reduced to below −140 dB/Hz in the 10 kHz to 10 MHz frequency range.
Beatnote Phase Noise	Higher phase noise with a broader noise pedestal.	Reduced phase noise with a narrower beatnote and lower pedestal.
Pump Laser Configuration	Multimode spatial distribution caused interference and reduced noise correlation.	Polarization-maintaining fibered polarization combiner used for single-mode fibers.
Semiconductor Structure	Unequal power distribution between the two lasing modes due to imbalance in losses	Adjusted pumping for balanced power distribution and symmetrical operation of lasing modes.

 doi:10.20944/preprints202604.0253.v1

Overall Noise Performance	Higher noise levels, unsuitable for precision applications.	Significantly improved noise performance, suitable for applications like microwave photonics.

A novel noise reduction architecture for dual-frequency VECSELs using correlated multimode pumping was demonstrated in [68]. This approach achieved a 10-20 dB reduction in RF beatnote phase noise over the 10 kHz-20 MHz range. The authors proposed a pumping scheme at 852 nm in which a laser diode beam was split to independently pump two modes, ensuring strong in-phase noise correlation and minimizing cross-saturation. This configuration reduced mode coupling and improved phase noise performance by optimizing pump overlap and correlation. The setup incorporated a half-VCSEL chip with quantum wells for efficient pump absorption and class-A dynamics, with orthogonally polarized modes separated by a birefringent crystal (Figure 1). Experimental results showed an 8-15 dB reduction in anti-phase noise compared to in-phase noise, confirming that low coupling constants and fully in-phase pumping effectively suppress gain competition. Correlation analysis indicated strong in-phase noise dominance, with correlation amplitudes exceeding 0.8 up to several MHz, validating the architecture's ability to suppress anti-phase noise. Additionally, the study explored dominant noise sources, identifying the Henry factor as a key contributor to high-frequency phase noise, while thermal fluctuations played a major role at lower frequencies. Although this architecture significantly reduced beatnote phase noise compared to single-spot pumping, further refinement of thermal noise modeling is necessary for improved accuracy at low frequencies. Table 8 provides a comparative summary of single-pump versus dual-pump architectures with in-phase correlated pumping for DF-VECSELs, highlighting their impact on phase noise and RIN reduction [65].

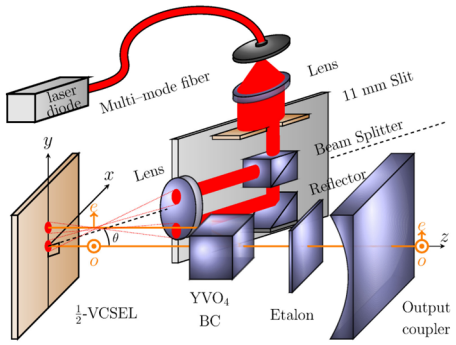

Figure 13. Experimental set-up for fully in-phase correlated pumping. The cross-polarized ordinary (o) wave and extraordinary (e) wave created by the birefringent crystal (BC) are separately pumped thanks to amplitude division of a multi–mode fibered laser diode [68]. Reproduced with permission from [68] copyright 2018, OPTICA.

Table 8. Comparison between Multimode fibered pump lasers and Single-mode fibered pump lasers for DF-VECSELs.

Aspect	Single-Pump Scheme	Dual-Pump Scheme (In-Phase Correlated)
Pump configuration	Single pump spot	Two spatially separated, in-phase correlated pumps
Coupling constant (C)	Higher, leading to stronger mode coupling	Low (C=0.05C), minimizing mode coupling
Beat note phase noise	Higher noise due to uncorrelated pump intensity	10-20 dB lower noise across 10 kHz–20 MHz

 doi:10.20944/preprints202604.0253.v1

Correlation amplitude (ξ)	Not fully correlated, ξ<1	Strong correlation, ξ≈1
Noise phase (ϕ)	Not optimized (ϕ≠0)	Fully in-phase (ϕ=0)
High-frequency noise (>1 MHz)	Dominated by phase-amplitude coupling noise	Phase-amplitude coupling noise eliminated
Low-frequency noise (<1 MHz)	Dominated by thermal fluctuations and technical noise	Still dominated by thermal fluctuations but reduced overall noise
Thermal noise modeling	Less reliant on pump correlation	Improved due to enhanced pump correlation
Noise suppression potential	Limited due to single-source configuration	Significant improvement, limited by thermal noise correlation
Pump configuration	Single pump spot	Two spatially separated, in-phase correlated pumps
Coupling constant (C)	Higher, leading to stronger mode coupling	Low (C=0.05C), minimizing mode coupling
Beat note phase noise	Higher noise due to uncorrelated pump intensity	10–20 dB lower noise across 10 kHz–20 MHz

5. Discussion

In the future, the transition of Dual-Frequency (DF) and Dual-Wavelength (DW) VECSELs from laboratory research to industrial infrastructure will be defined by their role as a universal, frequency-agile semiconductor platform. While both share the same high-power, external-cavity architecture, they serve distinct but complementary roles in the future technology ecosystem. The primary advantage of DF-VCESELs, is the exploitation of Class-A dynamical behavior. Unlike traditional solid-state lasers that suffer from relaxation oscillation noise, DF-VECSELs provide the ultra-pure microwave beat notes required for 6G network synchronization and compact CPT-based atomic clocks [69]. In the future, these will replace complex multi-laser setups with a single-chip source for jitter-free RF photonics.

On the other hand, the advantage of DW VECSELs, is the massive intracavity circulating power (hundreds of Watts), which drives efficient nonlinear frequency conversion. By generating two widely spaced wavelengths in one cavity, these devices enable Difference Frequency Generation (DFG) to reach the Mid-Infrared 'molecular fingerprint' region. This facilitates portable, high-sensitivity sensors for environmental monitoring and non-invasive diagnostics [40].

That's why, a review paper is essential now to map the evolution toward Membrane External-Cavity Surface-Emitting Lasers (MECSELs). This shift from modular mirror setups to monolithic 'semiconductor bricks' is the key hurdle for ruggedizing these lasers for the future field deployment in aerospace and mobile 6G base stations [70].

In addition to these capabilities, recent developments continue to demonstrate that VECSELs remain one of the most versatile semiconductor laser platforms. Their ability to deliver precise, application-specific wavelengths remains essential for fields such as atomic clocks, quantum computing, and free-space optical links [71], all of which rely on narrow-linewidth, stable, and tunable laser sources. Furthermore, studies highlight how VECSEL architectures naturally support multi-wavelength and frequency-agile operation, enabling simultaneous emission at several wavelengths for atomic and ionic species in advanced quantum systems [71]. These multi-line VECSEL platforms have been shown to provide high power, robustness, and environmental stability, underscoring the continued relevance of DF and DW designs in state-of-the-art quantum technologies. Meanwhile, breakthroughs in nonlinear conversion [72], such as record-brightness visible and mid-IR generation, underline that the intrinsic cavity power and flexible intracavity engineering of VECSELs will remain unmatched advantages moving forward. Together, these

 doi:10.20944/preprints202604.0253.v1

developments confirm that the dual-frequency and dual-wavelength VECSEL concepts reviewed here are not only scientifically relevant but represent key enabling technologies whose importance persists and will continue to grow as photonic systems demand higher spectral purity, wavelength agility, and integrable nonlinear functionality.

6. Conclusion

This review has summarized recent advancements in dual-wavelength VECSELs, emphasizing their increasing relevance for both scientific and industrial applications. After providing a historical perspective, it explored the core features that make VECSELs attractive, high brightness, excellent beam quality, wavelength tunability, and flexible design. The review examined key dual-wavelength configurations, including two-color VECSELs, systems based on separate chips, and dual-frequency (DF) designs. Each configuration offers distinct benefits, such as independent wavelength control or efficient frequency generation within a single cavity. Particular attention was given to the role of birefringent crystals and external-cavity architecture in achieving stable and tunable dual-wavelength emission. These innovations are paving the way for new applications in high-resolution spectroscopy, terahertz generation, and advanced optical systems. Continued research and integration efforts are expected to further enhance the performance and versatility of dual-wavelength VECSELs, reinforcing their role in the future of photonic technologies.

References

1. Gupta R. K., Handbook of Semiconductors: Fundamentals to Emerging Applications, 1st ed., CRC Press, **2024**,
2. Michalzik R., (ed) VCSELs: Fundamentals, Technology and Applications of Vertical-Cavity Surface-Emitting Lasers, Springer Series in Optical Sciences., Berlin, Vol. 166, **2012**.
3. Laurain A., Kilen I., Hader J., Perez A.R., Ludewig P., Stolz W., Addamane S., Balakrishnan G., Koch S.W., Moloney J.V. Modeling and Experimental Realization of Modelocked VECSEL Producing High Power Sub-100 Ps Pulses. *Appl Phys Lett* **2018**, *113*.
4. Lorenser D., Maas D.J.H.C., Unold H.J., Bellancourt A.-R., Rudin B., Gini E., Ebling D., Keller U. 50-GHz Passively Mode-Locked Surface-Emitting Semiconductor Laser with 100-mW Average Output Power. *IEEE J Quant Electron* **2006**, *42*, 838–847.
5. Scheller M., Wang T.-L., Kunert B., Stolz W., Koch S.W., Moloney J.V. Passively Modelocked VECSEL Emitting 682 Fs Pulses with 5.1 W of Average Output Power. *Electron Lett* **2012**, *48*.
6. Wilcox K.G., Tropper A.C., Beere H.E., Ritchie D.A., Kunert B., Heinen B., Stolz W. 4.35 kW Peak Power Femtosecond Pulse Mode-Locked VECSEL for Supercontinuum Generation. *Opt Express* **2013**, *21*, 1599–1605.
7. Jetter M., Michler P., Vertical External Cavity Surface Emitting Lasers: VECSEL Technology and Applications, 1st ed. Weinheim., **2021**,
8. Heinen, B, Wang, TL, Sparenberg, M, Weber, A, Kunert, B, Hader, J, Koch, SW, Moloney, JV, Koch, M, Stolz, W 106 W Continuous-Wave Output Power from Vertical-External-Cavity Surface-Emitting Laser. *Electron. Lett.* **2012**, *48*, 516–517.
9. Kuznetsov M. , Hakimi F., Sprague R., Mooradian A. , High-Power (>0.5-W CW) Diode-Pumped Vertical-External-Cavity Surface-Emitting Semiconductor Lasers with Circular TEM/Sub 00/ Beams. *IEEE Photonics Technol. Lett.* **1997**, *9*, 1063–1065.
10. Hader, J., Hardesty, G., Hardesty, G., Yarborough, M. J., Kaneda, Y., Moloney, J. V., Kunert, B., Stolz, W., Koch, S. W. Predictive Microscopic Modeling of VECSELs. *IEEE J Quantum Elec* **2010**, *46*, 810–817.
11. Y. Kaneda, JM. Yarborough, L. Li,N. Peyghambarian, L. Fan et al. Continuous-Wave All-Solid-State 244 Nm Deep-Ultraviolet Laser Source by Fourth-Harmonic Generation of an Optically Pumped Semiconductor Laser Using CsLiB6O10 in an External Resonator. *Opt Lett* **2008**, *33*.
12. Scheller, M., Yarborough, J. M., Moloney, J. V., Fallahi, M., Koch, M., Koc, S. W. Room Temperature Continuous Wave Milliwatt Terahertz Source. *Opt Express* **2010**, *18*.

 doi:10.20944/preprints202604.0253.v1

13. Paul, J. R., Scheller, M., Laurain, A., Young, A., Koch, S. W., Moloney, J. Narrow-Linewidth Single-Frequency Terahertz Source Based on Difference Frequency Generation of Verticalexternal-Cavity Surface-Emitting Lasers in an External Resonance Cavity. *Opt Lett* **2013**, *38*.
14. Underer, T., Northrup, J. E., Yang, Z., Teepe, M., Strittmatter, A., Johnson, N. M., Rotella, P., Wraback, M. In-Well Pumping of InGaN/GaN Vertical-External-Cavity Surfaceemitting Lasers. *Appl Phys Lett* **2011**, *99*.
15. Kuznetsov, M. VECSEL Semiconductor Lasers: A Path to High-Power, Quality Beam and UV to IR Wavelength by Design. In *Semiconductor Disk Lasers: Physics and Technology*, pp. 1–71, **2010.**
16. Rahim, M., Arnold, M., Felder, F., Behfar, K., Zogg, H. Midinfrared Lead-Chalcogenide Vertical External Cavity Surface Emitting Laser with Wavelength. *Appl Phys Lett* **2007**, *91*.
17. H. Lindberg, A. Strassner, E. Gerster, A. Larsson 0.8 W Optically Pumped Vertical External Cavity Surface Emitting Laser Operating CW at 1550 Nm. *Electron Lett* **2004**, *40*, 601–602.
18. Butkus, M., Rautiainen, J., Okhotnikov, O. G., Hamilton, C. J., Malcolm, G. P. A., Mikhrin, S. S., Krestnikov, I. L., Livshits, D. A., Rafailov, E. U. Quantum Dot Based Semiconductor Disk Lasers for 1–1.3 Mm. *IEEE J Sel Top Quantum Electron* **2011**, *17*, 1763–1771.
19. Rantamäki, A., Sokolovskii, G. S., Blokhin, S. A., Dudelev, V. V., Soboleva, K. K., Bobrov, M. A., Kuzmenkov, A. G., et al. Quantum Dot Semiconductor Disk Laser at 1.3 Mm. *Opt Lett* **2015**, *40*, 3400–3403.
20. Zakharian A R., Hader J., Moloney J V., Koch S W, Brick P, Lutgen S Experimental and Theoretical Analysis of Optically Pumped Semiconductor Disk Lasers. *Appl Phys Lett* **2003**, *83*, 1313–1315.
21. Kemp A.J, Valentine G.J, Hopkins J.M, Hastie J.E, Smith S.A, Calvez S. Thermal Management in Vertical-Externalcavity Surface-Emitting Lasers: Finite-Element Analysis of a Heatspreader Approach. *IEEE J Quantum Electron 41*, 148–155.
22. Wang F., Wang X., Wang J., Wei Z., Fang D., Fang X. Thermal Analysis of 980 Nm Optically Pumped Verticalexternal- Cavity Surface Emitting Lasers with DBM Structure: Finite Element Method. *Opt-Int J Light Electron Opt* **2012**, *124*, 2897–2900.
23. Saarinen E J., Puustinen J., Sirbu A., Mereuta A., Caliman A.,Kapon E., Okhotnikov O G. Power-Scalable 1.57 Mmmode-Locked Semiconductor Disk Laser Using Wafer Fusion. *Opt.Lett.* **2009**, *34*, 3139–3141.
24. Bek R., Kahle H., Schwarzbäck T., Jetter M., Michler P. Mode-Locked Red-Emitting Semiconductor Disk Laser with Sub-250 Fs Pulses. *Appl Phys Lett* **2013**, *103*.
25. Heinen B., Moller C., Jandieri K., Kunert B., Koch M., Stolz W. The Thermal Resistance of High-Power Semiconductor Disklasers. **2015**, *51*, 1–9.
26. Bondaz T A G., Laurain A., Moloney J V., McInerney J G. Generation and Stabilization of Continuous-Wave THz Emission From a Bi-Color VECSEL. In Proceedings of the Proc. SPIE 11263, 2020.
27. Scheller M., Baker C. W., Koch S. W., Moloney J. V. , Jason Jones R. High Power Dual-Wavelength VECSEL Based on a Multiple Folded Cavity. *IEEE Phot Techn Lett* **2017**, *29*, 790–793.
28. Guoyu H., Kriso C., Zhang F., Wichmann M., Stolz W., Fedorova KA., Rahimi-Iman A. Two-Chip Power-Scalable THz-Generating Semiconductor Disk Laser. *Opt Lett* **2019**, *44*, 4000–4003.
29. Lukowski, M., Hessenius C., Meyer J., Fallahi, M. Over 10 Watt, Collinear Blue and Green Vertical External Cavity Surface Emitting Laser. In Proceedings of the Proc. SPIE, San Francisco, 2016, Vol. 9734.
30. Camargo F., Girard N., Danet J., Baili G., Morvan L. , Dolfi D. , Holleville D, Guérandel S, Sagnes I., Georges P. , Lucas-Leclin G. Tunable High-Purity Microwave Signal Generation from a Dual-Frequency VECSEL at 852 Nm. *Proc. SPIE—Int. Soc. Opt. Eng.* **2013**.
31. Chaccour L., Aubin G., Merghem K., Jean-Louis Oudar J-L., Khadour A., Chatellier P., Bouchoule S.," Cross-Polarized Dual-Frequency VECSEL at 1.5 Mm for Fiber-Based Sensing Applications. *IEEE Phot Joournal* **2016**, *8*, 1–10.
32. Grischkowsky D., Keiding S., Van Exter M., Fattinger Ch., Far-Infrared Time-Domain Spectroscopy with Terahertz Beams of Dielectrics and Semiconductors. *J Opt Soc Amer B Opt Phys 7*, 2006–2015.
33. Siegel P., Terahertz Technology in Biology and Medicine. *IEEE Trans Microw Theory Techn* **2004**, *52*, 2438–2447.
34. Federici J., Schulkin B., Huang F., Gary D., Barat R., Oliveira F., Zimdars D. THz Imaging and Sensing for Security Applications—Explosives, Weapons and Drugs. *Semicond Sci Technol* **2005**, *20*, 266.

 doi:10.20944/preprints202604.0253.v1

35. Song H., Nagatsuma T. Present and Future of Terahertz Communications. *IEEE Trans Terahertz Sci Technol* **2011**, *1*, 256–263.
36. Scheller M., Koch SW., Moloney JV. Grating-Based Wavelength Control of Single- and Two-Color Vertical-External-Cavity-Surface-Emitting Lasers. *Opt Lett* **2012**, *37*, 25–27.
37. Scheller M., Baker C. W., Koch S. W., Moloney J. V. , Jason Jones R. High Power Dual-Wavelength VECSEL Based on a Multiple Folded Cavity. *IEEE Phot Techn Lett* **2017**, *29*, 790–793.
38. S. L. Tsai, C. Y. Cho Generating Dual-Wavelength VECSEL by Selecting Birefringence Filter Material and the Application toward Mid-Infrared Region via Intracavity OPO. *Opt Express* **2023**, *31*, 24555–24565.
39. Tsaoussis S. P., Addamane S., Jones R. J., Moloney J. V. Dual-Wavelength Channel GHz Repetition Rate Mode-Locked VECSEL Cavities Sourced from a Common Gain Medium. *Opt Lett* **2024**, *49*, 1688–1691.
40. Zhang Z., Zhang J., Du Z., Bai H., Zhang J., Liu T., Zhou Y., Zhang X., Chen C., Qin L. et al. Single-Chip Switchable Dual-Wavelength Vertical External-Cavity Surface-Emitting Laser. *Crystals* **2023**, *23*.
41. Li Z., Zhang J., Zhang X., Zhang Z., Zhou Y., Ning Y. Nanosecond Pulse Generation in Optically Pumped Dual-Wavelength Vertical-External-Cavity Surface-Emitting Laser. *IEEE Phot Joournal* **2022**, *14*, 1–6.
42. Abbes A., Lu P.-K., Nouvel P., Pénarier A., Varani L., Beaudoin G. 280 GHz Radiation Source Driven by a 1064 nm Continuous-Wave Dual-Frequency Vertical External Cavity Semiconductor Laser., Chengdu, China, 2021.
43. Liu H.-Y., Ma H.-D., Bian Q., Bo Y., Cui D.-F., Peng Q.-J. Microsecond Pulsed Yellow Emission by Intracavity Doubled Optically Pumped Two-Chip VECSEL. *Laser Phys Lett* **2023**, *20*.
44. Scheller M., Paul J. R., Laurain A., Young A., Koch S. W., Moloney J. V. Terahertz Generation by Difference Frequency Conversion of Two Single-Frequency VECSELs in an External Resonance Cavity. In Proceedings of the SPIE LASE, San Francisco, 2014, Vol. 8966.
45. Hessenius C., Lukowski M., Fallahi M. High-Power Tunable Two-Wavelength Generation in a Two Chip Co-Linear T-Cavity Vertical External-Cavity Surface-Emitting Laser. *Appl Phys Lett* **2012**, *101*, 121110-1-121110–121113.
46. Lukowski M., Hessenius C., and Fallahi M. Widely Tunable High-Power Two-Color VECSELs for New Wavelength Generation. *IEEE J Sel Top Quantum Electron* **2015**, *21*.
47. Zhang F., Gaafar M., Möller C., Stolz W., Koch M., Rahimi-Iman A. A Serially-Connected Two-Chip VECSEL for Dual-Wavelength Emission., St. Petersburg, 2016.
48. Zhang F., Gaafar M., Möller C., Stolz W., Koch M., Rahimi-Iman A. Dual-Wavelength Emission From a Serially Connected Two-Chip VECSEL. *IEEE Phot Tech Lett* **2016**, *28*, 927–929.
49. Baili G., Bretenaker F., Alouini M., Morvan L., Dolfi D., Sagnes I. Experimental Investigation and Analytical Modeling of Excess Intensity Noise in Semiconductor Class-A Lasers. *J Light. Technol* **2008**, *26*, 952–961.
50. Capmany J., Novak D. Microwave Photonics Combines Two Worlds. *Nat Photonics* **2007**, *1*, pages319-330.
51. Brévalle G., Pes S., Paranthoën C., Perrin M., Levallois C., Hamel C., Mereuta A., Caliman A., Kapon E., Vallet A., Chusseau L., Folliot H., Alouini M. Direct Measurement of the Spectral Dependence of Lamb Coupling Constant in a Dual Frequency Quantum Well-Based VECSEL. *Opt Express* **2019**, *27*, 21083–21091.
52. Brévalle G., Pes S., Paranthoën C., Perrin M., Levallois C., Hamel C. Mode Coupling Measurement in Dual-Frequency Quantum Well-Based VECSEL., Nara, Japan, **2019**.
53. Pal V. , Trofimoff P. , Miranda B.-X., Baili G. , Alouini M. , Morvan L. , Dolfi D., Goldfarb F. , Sagnes I. , Ghosh R., Bretenaker F. Measurement of the Coupling Constant in a Two-Frequency VECSEL. *Opt. Express.* **2010**, *18*, 5008–5014.
54. Baili G., Morvan L., Alouini M., Dolfi D., Bretenaker F., Sagnes I., Garnache A. Experimental Demonstration of a Tunable Dual-Frequency Semiconductor Laser Free of Relaxation Oscillations. *Opt Lett* **2009**, *34*, 3421–3423.
55. Barrientos-Barria J., Camargo F., Janicot S., Sagnes I., Garnache A., Baili G., Morvan L., Georges P., Lucas-Leclin G. Dual-Frequency Operation of a Vertical External Cavity Semiconductor Laser for Coherent Population Trapping Cesium Atomic Clocks., **2011**.
56. Dumont P., Danet JM., Holleville D., Guérandel S., Baili G., Morvan L., Pillet G., Dolfi D., Gozhyk I., Beaudoin G., Sagnes I., Georges P., Lucas-Leclin G.. Evaluation of the Noise Properties of a Dual-Frequency VECSEL for Compact Cs Atomic Clocks. In Proceedings of the Proc SPIE., San Francisco, **2015**, Vol. 9349.

 doi:10.20944/preprints202604.0253.v1

57. Cotxet J., Gutty F., Baili G., Morvan L., Dolfi D. Guérandel S. Laser Power Stabilization of a Compact Dual-Frequency VECSEL for a Cesium Clock Optical Bench., Versailles, France., **2022**.
58. Cotxet J., Gutty F., Baili G., Morvan L., Dolfi D., Holleville D., Guerandel S. An Innovative Laser Bench for a High-Performance Compact Cesium CPT Clock. In Proceedings of the Proc SPIE., Dubrovnik, Croatia, 2022.
59. Chaccour L., Aubin G., Merghem K., Oudar J-L., Khadour A., Chatellier P., Bouchoule S. Dual-Frequency VECSEL at Telecom Wavelength for Sensing Applications., Lisbon, Portugal., **2016**, pp. 53–58.
60. Liu H., Gredat G., De S., Fsaifes I., Ly A., Vatré R. Noise Reduction in a Dual-Frequency VECSEL at Telecom Wavelength Using Fully Correlated Pumping., Toulouse, France., **2018**.
61. Gredat G., Liu H., Cotxet J., Tricot F., Baili G., Gutty F., Goldfarb F., Sagnes I., Bretenaker F. Optimization of Laser Dynamics for Active Stabilization of DF-VECSELs Dedicated to Cesium CPT Clocks. *J Opt Soc Am B* **2020**, *37*, 1196–1207.
62. Liu H., Goldfarb F., Guerchi N., Chow C-H., Bretenaker F., Dumont P., Lucas-Leclin G., Baili G., Sagnes I., Beaudoin G. Noise Measurement and Modeling of a Dual-Frequency VECSEL at Cesium Clock Wavelength., Paris, France, **2017**.
63. Liu H., Gredat G., Baili G., Gutty F., Goldfarb F., Sagnes I., Bretenaker F. Noise Investigation of a Dual-Frequency VECSEL for Application to Cesium Clocks. *J Light. Technol 36*, 3882–3891.
64. De S., Pal V., El Amili A., Pillet G., Baili G., Alouini M., Sagnes I., Ghosh R., Bretenaker F. Intensity Noise Correlations in a Two-Frequency VECSEL. *Opt Express* **2013**, *21*, 2538–5250.
65. Liu H., Gredat G., De S., Fsaifes I., Ly A., Vatré R., Baili G., Bouchoule S., Goldfarb F., Bretenaker F. Ultra-Low Noise Dual-Frequency VECSEL at Telecom Wavelength Using Fully Correlated Pumping. *Opt Lett* **2018**, *43*, 1794–1797.
66. De S., El Amili A., Fsaifes I., Pillet G., Baili G., Goldfarb F., Alouini M., Sagnes I., Bretenaker F. Phase Noise of the Radio Frequency Beatnote Generated by a Dual-Frequency VECSEL., USA, **2013**, pp. 52–55.
67. De S., Baili G., Bouchoule S., Alouini M., Bretenaker F. Intensity- and Phase-Noise Correlations in a Dual-Frequency Vertical-External-Cavity Surface-Emitting Laser Operating at Telecom Wavelength. *Phys Rev A* **2015**, *91*.
68. Gredat G., Chatterjee D., Baili G., Gutty F., Sagnes I., Goldfarb F., Bretenaker F., Liu H. Fully–Correlated Multi–Mode Pumping for Low–Noise Dual–Frequency VECSELs. *Opt Express* **2018**, 20.
69. Karuseichyk S., Pal V., Sahoo S., Beaudoin G., Sagnes I., Bretenaker F. Investigation of Noise Correlations in the Phase-Locked Class-A VECSEL Array. **2023**, *31*, 41713–41725.
70. Kahle H., Tatar-Mathes P., Rajala P., Mircea G., Membrane External-Cavity Surface-Emitting Lasers (MECSELs): State of the Art in Broadband (> 25 THz) Tuning and Antiresonant Gain Structure Design., Strasbourg, France, **2022**.
71. Compound Semiconductor. Vexlum Raises €10m to Scale Laser Fabrication. 2024. Available online: https://compoundsemiconductor.net/article/123488/Vexlum_raises_%E2%82%AC10m_to_scale_laser_fabrication (accessed on March 2026).
72. Vertical Cavity Surface-Emitting Laser (VCSEL) Global Market Report, The Business Research Company: London, UK, **2026**.